HYDROLOGIC DISTURBANCES

THE ORIGIN OF THE TSUNAMI EXCITED BY THE EARTHQUAKE—FAULTING OR SLUMPING

By Kuo-Fong Ma, California Institute of Technology,
Kenji Satake, University of Michigan,
and
Hiroo Kanamori, California Institute of Technology

CONTENTS

ABSTRACT

The first arrival of the tsunami recorded at Monterey, California, was about 10 min after the origin time of the earthquake. Using an elastic half space, we computed vertical ground displacements for many different fault models for the Loma Prieta earthquake and used them as the initial condition for computation of the tsunami in Monterey Bay. The synthetic tsunami computed for the uniform dislocation model determined from seismic data can explain the arrival time, polarity, and amplitude of the beginning of the tsunami. However, the period of the synthetic tsunami is too long compared with the observed. We tested other fault models with more localized slip distribution. None of the models could explain the observed period. The residual waveform, the observed minus the synthetic waveform, begins as a downward motion at about 18 min after the origin time of the earthquake and could be interpreted as due to a secondary source near Moss Landing. If the large-scale slumping near Moss Landing suggested by an eyewitness observation occurred about 9 min after the origin time of the earthquake, it could explain the residual waveform. To account for the amplitude of the observed tsunami, the volume of sediments involved in the slumping is approximately 0.012 km^3. Thus the most likely cause of the tsunami observed at Monterey is the combination of the vertical uplift of the sea floor due to the main faulting and a large-scale slumping near Moss Landing.

INTRODUCTION

The Loma Prieta earthquake (M_W=6.9) generated a tsunami in Monterey Bay, just south of the epicenter (fig. 1*A*). Such nearfield tsunamis are relatively rare in the United States; the 1906 San Francisco earthquake (Lawson, 1908), the 1927 Lompoc earthquake, the 1964 Alaskan earthquake, and the 1975 Kalapana earthquake are among the few examples. Since large coastal earthquakes, either onshore or offshore, can cause serious tsunami hazards, we investigated the tsunami excited by the Loma Prieta earthquake in an attempt to understand the generation mechanism of such nearfield tsunamis. We will show that two elements contributed to tsunami excitation—the vertical deformation of the sea floor caused by faulting and the secondary submarine slumping presumably caused by shaking.

DATA

The tsunami was recorded (fig. 1*B*) on the tide gauge in Monterey Bay. Schwing and others (1990) described this instrument as a bubble gauge. We digitized and detrended the record (fig. 1*C*) for one hour starting from the origin time of the earthquake. The first arrival of the tsunami is about 10 minutes after the origin time of the earthquake, and the peak-to-peak amplitude is about 40 cm.

METHOD

Tsunami waveforms are computed either analytically for the case of uniform depth (see Takahashi, 1942; Kajiura, 1963; Ward, 1982; Comer, 1984; Okal, 1988) or numerically for actual bathymetry (Hwang and others, 1972; Houston, 1978; Aida, 1978; Satake, 1985). Since the bathymetry in Monterey Bay (fig. 2) is very complex—a canyon runs northeast to southwest—an assumption of uniform depth is not valid. We used a finite difference method to compute the tsunami in the bay using the actual bathymetry, which is known very accurately.

As the initial condition for tsunami computation, we used the vertical ground displacement caused by faulting. For this computation, we used Okada's (1985) program, which computes ground deformation caused by faulting in a homogeneous half space. Since the source process time of the earthquake is less than 10 seconds and the water depth is much smaller than the scale length of the ground deformation, we assumed that the water surface is uplifted instantaneously exactly in the same way as the bottom deformation. The amplitude of the tsunami is of the order of 10 cm and is much smaller than the water depth, about 100 m. Also, the wavelength of the tsunami, about 10 km in the bay, is much longer than the water depth. Hence we can use the vertically integrated linear long-wave equation and continuity equation as basic equations of tsunami propagation. In a Cartesian coordinate system (x, y) these equations are given by

$$\frac{\partial Q_x}{\partial t} = -gD\frac{\partial H}{\partial x}$$

$$\frac{\partial Q_y}{\partial t} = -gD\frac{\partial H}{\partial y}$$

and

$$\frac{\partial H}{\partial t} = -\frac{\partial Q_x}{\partial x} - \frac{\partial Q_y}{\partial y} \quad , \qquad (1)$$

where Q_x and Q_y are the flow rate obtained by integrating the velocity vertically from the bottom to the surface in the x and y directions respectively, g is the acceleration of gravity, D is the water depth, and H is the water height above the average surface. These equations are solved with a finite difference method. The bathymetry in Monterey Bay and the area for which the computation is made are shown in figure 2. The grid size is 1/4 min, which is about 400 m and 500 m in the x and y directions, respectively, and the number of grid points is about 14,400. The time step of computation is 2 s, which is chosen to satisfy the stability condition for the finite difference calculation. Since the bathymetry is known in detail, the tsunami can be computed very accurately.

FAULT MODEL

The fault model of the Loma Prieta earthquake has been determined very accurately using seismic, geodetic, and

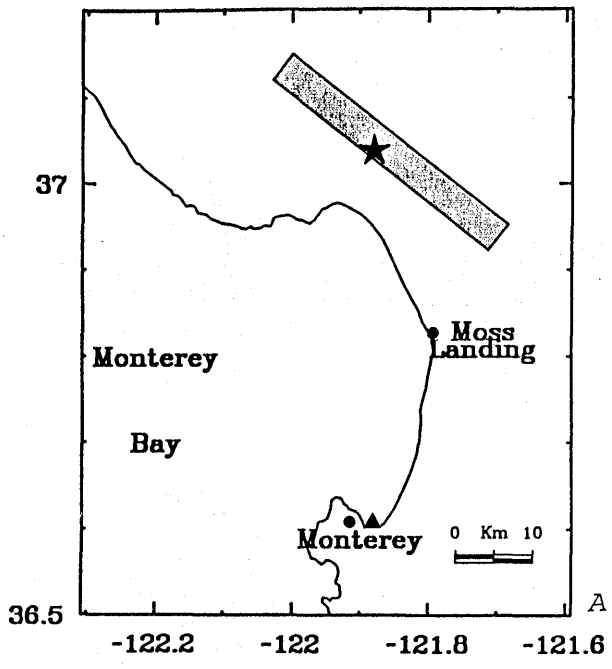

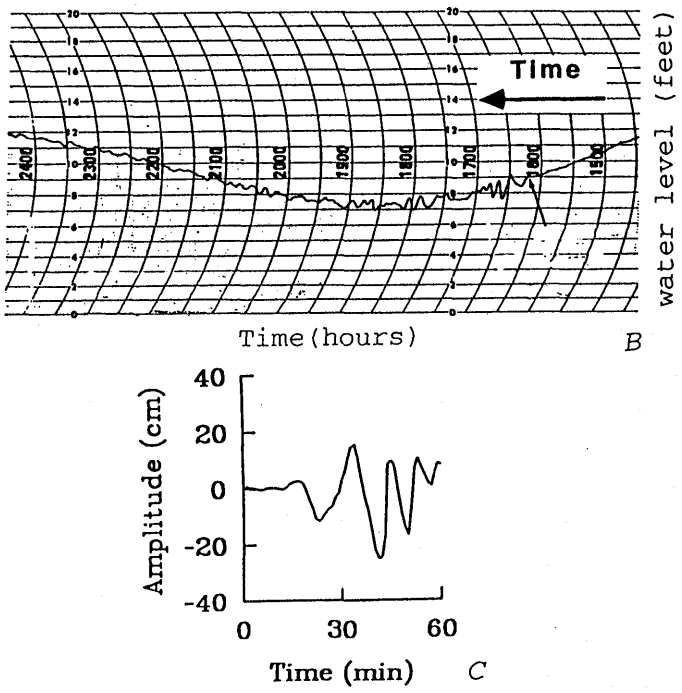

Figure 1.—*A*, Locations of earthquake epicenter (star) and fault (shaded strip) and tide gauge station (solid triangle). *B*, Tsunami record from tide gauge at Monterey (after Schwing and others, 1990). *C*, Detrended tsunami record for one hour starting from origin time of earthquake.

aftershock data. Kanamori and Satake (1990) inverted teleseismic body- and surface-wave data and obtained a mechanism with dip=70° SW., rake=138°, and strike=N. 128° E. The seismic moment is 3×10^{26} dyne-cm (M_W=6.9). The total length of the aftershock area is about 40 km, and the main shock is located near the center of the aftershock (U.S. Geological Survey Staff, 1990), which suggests bilateral faulting. Kanamori and Satake (1990) suggested a uniform fault model having a fault length, L, of 35 km. The coseismic slip on the fault is 238 cm, if the fault width, W, is assumed to be 12 km. Lisowski and others (1990) compared the observed geodetic data with several dislocation fault models; their preferred fault model has a fault length of 37 km and fault width of 13.3 km. The coseismic slip on the fault is 204 cm. The focal mechanism has dip=70° SW., rake=144°, and strike=N. 44° W. The total seismic moment determined from geodetic data is the same as that determined from seismic data by Kanamori and Satake (1990).

RESULTS

We first computed the vertical crustal deformation for the uniform seismic fault model (L=35 km, W=12 km, and D=238 cm) determined by Kanamori and Satake (1990) and used it as the initial condition for tsunami computation. Figure 3*A* shows the location of the epicenter and the vertical crustal deformation. The displacement beneath the sea floor, a maximum of 25 cm, was responsible for tsunami generation.

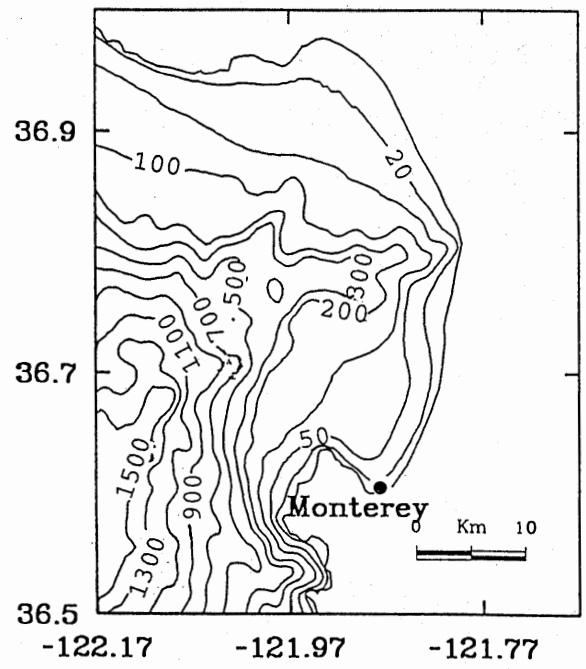

Figure 2.—Bathymetry in Monterey Bay and area over which tsunami computation was made. Contour lines indicate water depths in meters (contour intervals are variable).

To see the contribution of the sea-floor displacement to the observed tsunami, we computed an inverse travel-time

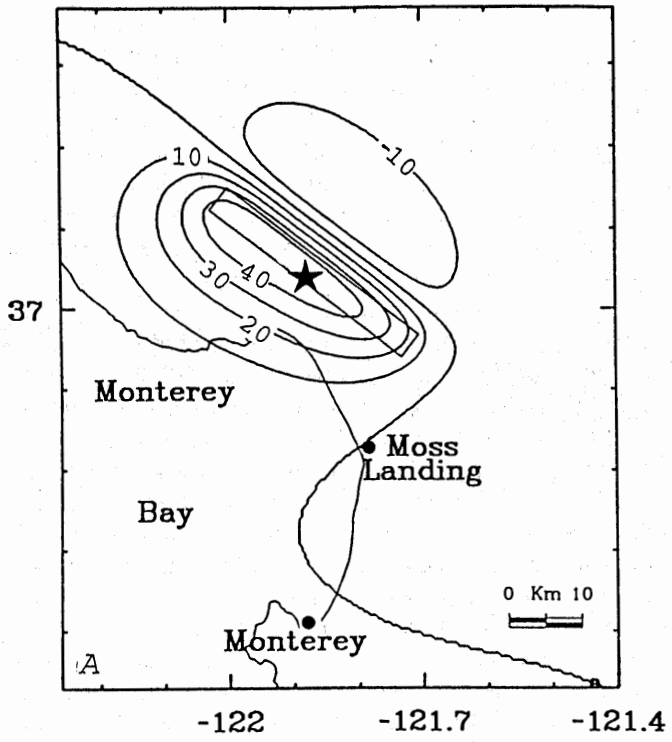

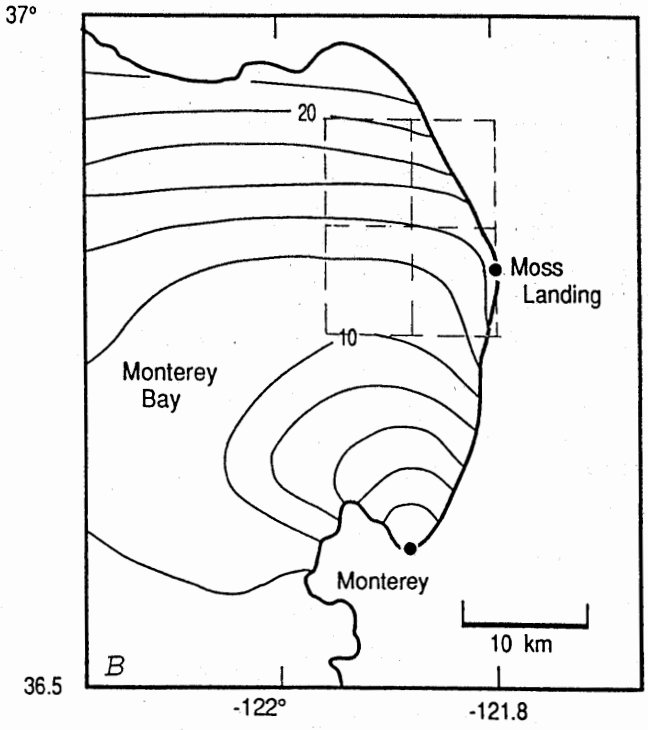

Figure 3.—*A*, Vertical crustal deformation with 10-cm contour intervals for uniform seismic fault model (L=35 km, W=12 km, and D=238 cm); earthquake epicenter indicated by asterisk. *B*, Inverse tsunami travel-time isochrons (contours indicate tsunami wavefronts at every 2 min); dashed box indicates area for inversion computation (see text for discussion).

diagram by placing a source at the tide-gauge station and propagating tsunamis backward into the bay. Figure 3*B* shows the inverse tsunami travel-times every 2 min. The isochron at 10 min is close to the south edge of the displacement field defined by the 0 cm contour line. This is consistent with the onset time of the tsunami at 10 min after the origin time of the earthquake. Figure 4 shows the snapshots of computed tsunamis at 5, 10, 15, 20, 25, and 30 min after the origin time.

Figure 5*A* compares the synthetic tsunami computed for this model with the observed. The synthetic tsunami can explain the arrival time, polarity, and amplitude of the beginning of the observed tsunami. However, the period of the synthetic tsunami is too long compared with the observed.

The reason for the long period of the synthetic tsunami is that the sea floor deformation caused by faulting is very broad. If the slip on the fault is more localized than that in the model used in the above computation, the period of the synthetic tsunami could be decreased. To test this, we computed tsunamis for three localized sources and for the geodetic fault model obtained by Lisowski, Prescott, Savage, and Johnston (1990) for comparison.

In the first case we localized the entire slip in the northwest half of the fault (fault length=17.5 km). In the second case, the slip is localized in the southeast half (fault length=17.5 km). In the third case, we localized the displacement in the bottom half of the fault plane (fault length=35 km, width=6 km). In all cases, the seismic moment is the same as for the uniform model. These cases represent the three extreme cases of localized sources. The fourth model is taken from Lisowski, Prescott, Savage, and Johnston (1990). Figures 5*B-E* compare the synthetics for these cases with the observed. The waveform of the synthetics is not very different from that for the uniform model. This result indicates that the displacement field caused by faulting is smoothed out in Monterey Bay, and it is not possible to explain the short period of the observed tsunami.

The difference in the period suggests that a secondary source may be responsible for the tsunami observed at

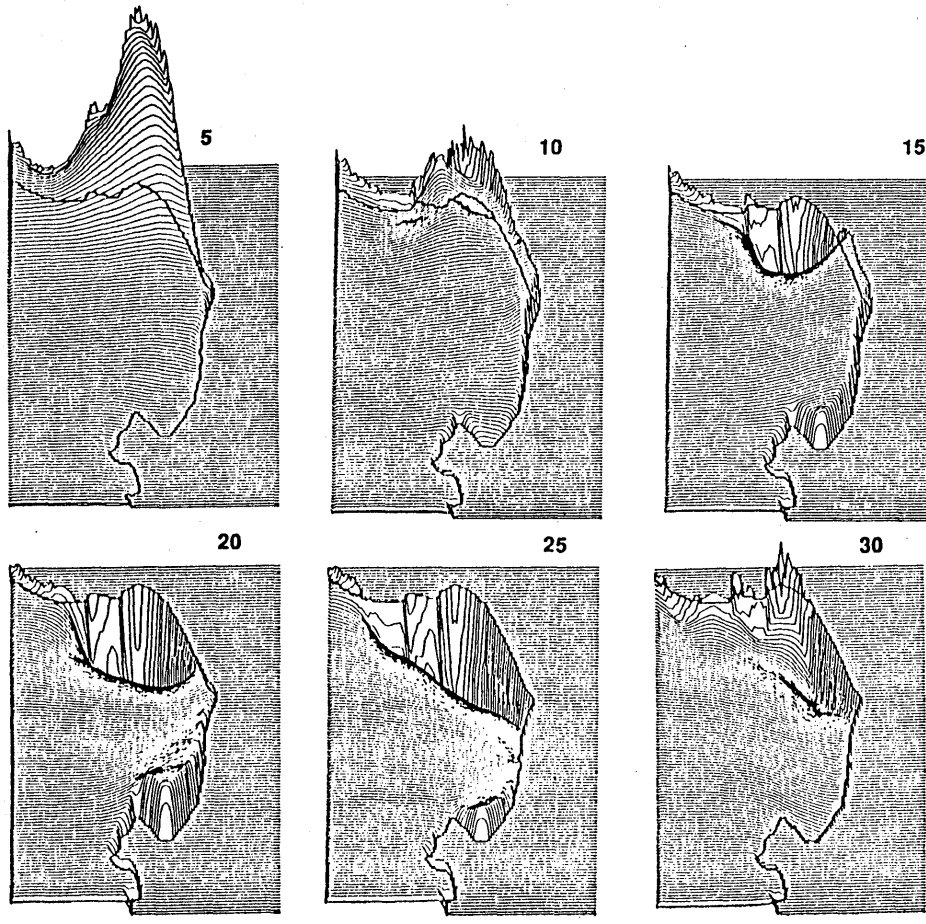

Figure 4.—Snapshots of the computed tsunami computed for the fault model at 5, 10, 15, 20, 25, and 30 min.

Monterey. To explore this possibility, we computed the residual waveform; that is, the observed minus the synthetic waveforms. The residual waveform, shown in figure 5*F*, begins as a downward motion at about 18 min after the origin time of the earthquake. Figure 3*B* shows that the isochron at 18 min is slightly north of Moss Landing. Schwing, Norton, and Pilskaln (1990) suggested the possibility of large-scale slumping near Moss Landing. Sea level fell by 1 m or more near Moss Landing soon after the earthquake. This sea level change is larger than the change expected solely from the direct effect of faulting. The inverse travel-time curve shown in figure 3*B* suggests that if this slumping occurred 9 min after the earthquake, the arrival time of the residual tsunami shown in figure 5*F* could be interpreted as due to the slumping at Moss Landing.

To determine more details of the secondary source responsible for the tsunami, we divided the sea floor into four blocks (8×10 km^2 each) as shown in figure 3*B*. Owing to the time delay of the secondary source, we shifted the residual waveform by 9 min and inverted the shifted residual tsunami waveform to determine the displacement for each block. The inversion is formulated as

$$A_j(t_i)\, x_j = b_j(t_i) \qquad (2)$$

where $A_j(t_i)$ is the tsunami amplitude at time t_i due to a unit displacement at the jth block, x_j is the displacement at the jth block, and $b_j(t_i)$ is the observed tide gauge record at time t_i. The displacement x_j for each block is estimated with a linear least squares inversion of equation (2).

Figure 6*A* shows the vertical displacement of the sea floor determined by the inversion. The displacement shows an isolated subsidence at the southeast block near Moss Landing, which is consistent with our assumption. The synthetic tsunamis computed for the displacement field shown in figure 6*A* and for a subsidence in the southeast block only are shown in figure 6*B* and 6*C*, respectively. Both can explain the period and the amplitude of the shifted residual tsunami. The southeast block near Moss Landing has a subsidence of about 15 cm over an area of 80 km^2. Figure 6*D* compares the synthetic waveform computed for faulting and slumping combined with the observed.

A slump may be most adequately modeled by a sudden subsidence followed by a gradual uplift. However, the details are unknown. If the later uplift was gradual, the tsunami source could be modeled using a single subsidence source. If this is the case, our result suggests that the volume of sediments involved in the slumping is approximately 0.013 km^3. However, this estimate depends on the details of the slumping. Unfortunately, from the single observation we cannot determine further details.

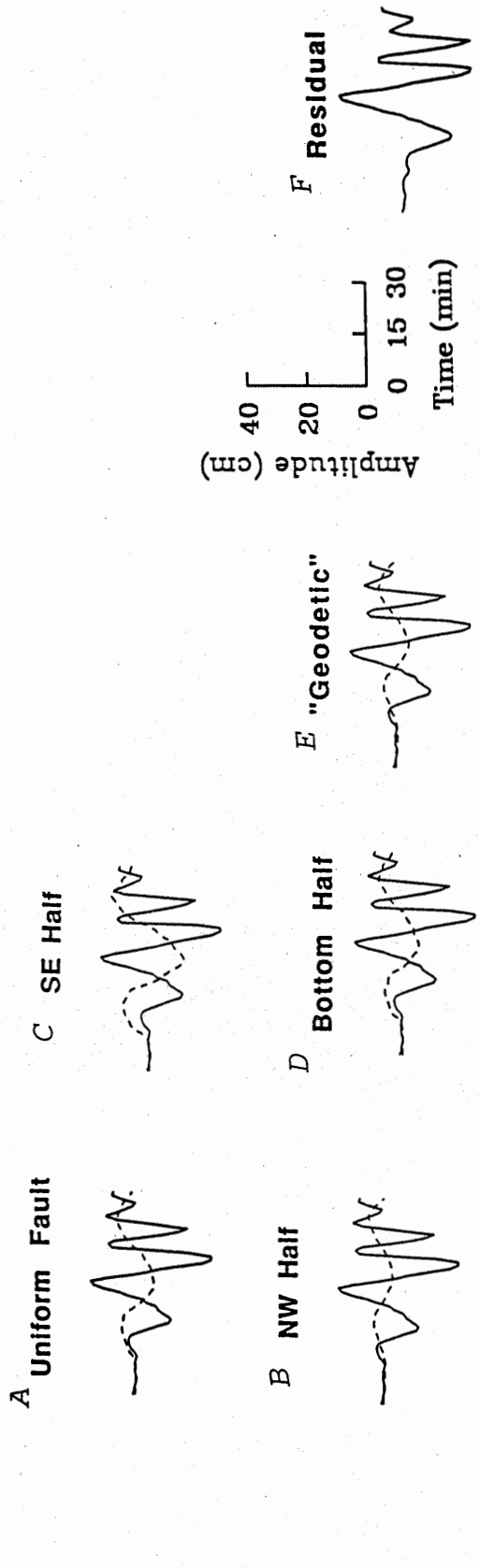

Figure 5.—*A–E*, Comparison of synthetic tsunami (dashed line) computed for various fault models with the observed tsunami (solid line). *F*, Residual waveform (observed minus synthetic waveform for uniform fault model).

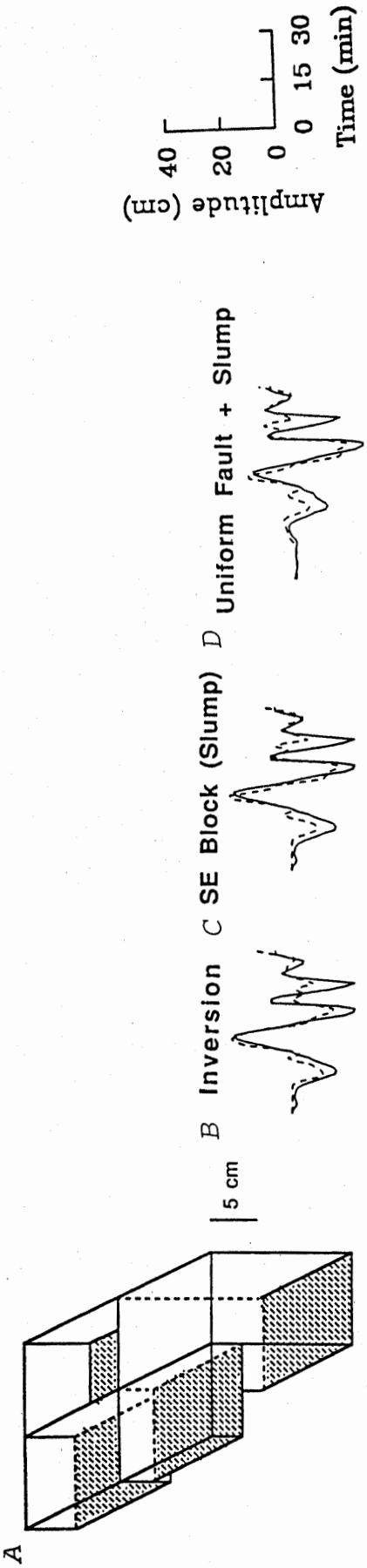

Figure 6.—*A*, Sea-floor displacement obtained from the inversion of observed tsunami. *B–C*, Comparison of residual waveform (solid line) with synthetic (dash line) for the displacement field obtained from inversion and computed for a 15-cm subsidence at southeast block (shown in *A*). *D*, Comparison of synthetic tsunami (dashed line) computed for faulting and slumping combined with observed (solid line).

CONCLUSIONS

The uniform fault model determined from seismic data can explain the arrival time, polarity, and amplitude of the beginning of the observed tsunami, but the period of the synthetic tsunami is too long. We tested fault models with a wide range of nonuniform slip distribution, but none of them could explain the observed period satisfactorily. This suggests that a secondary source is required to explain the tsunami observed at Monterey. The residual waveform, the observed minus synthetic waveform computed for the seismic source, suggests that the most likely secondary source is a sediment slump near Moss Landing; evidence for such a slump has been reported by an eyewitness.

Since the tsunami excited by the secondary source can be more extensive than that by the earthquake faulting itself, as is the case for the Loma Prieta earthquake, the possibility of tsunamis caused by secondary sources needs to be carefully evaluated in assessing the tsunami potential of nearshore earthquakes.

Acknowledgments.—This work was supported by National Science Foundation grant EAR 89-15987 and U.S. Geological Survey grant 14-08-0001-G1832. Contribution No. 4949, Division of Geological and Planetary Sciences, California Institute of Technology, Pasadena, California.

REFERENCES CITED

Aida, I., 1978, Reliability of a tsunami source model derived from fault parameters: Journal of Physics of the Earth, v. 26, p. 57-73.

Comer, R.P., 1984, The tsunami mode of a flat earth and its excitation by earthquake sources: Journal of the Royal Astronomical Society, v. 77, p.1-27.

Houston, J.R., 1978, Interaction of tsunamis with the Hawaiian Islands calculated by a finite-element numerical model: Journal of Physics of the Ocean, p. 93-102.

Hwang, L.-S., Butler, H.L., and Divoky, D.J.,1972, Tsunami model: Generation and open-sea characteristics: Bulletin of Seismological Society of America, v. 62, p. 1579-1596.

Kajiura, K., The leading wave of a tsunami, 1963: Bulletin of Earthquake Research Institute, University of Tokyo, v. 41, p. 535-571.

Kanamori, H., and Satake, K., 1990, Broadband study of the 1989 Loma Prieta earthquake: Geophysical Research Letter, v. 17, p. 1179-1182.

Lawson, A.C., Gilbert, G.K., Reid H.F., Branner, J.C, Leuschner, A.O., Davidson, G., Burkhalter, C., and Campbell, W.W., 1908, The California earthquake of April 18, 1906: report of the state earthquake investigation commission: Carnegie Institution, v. 2, p. 369-373.

Lisowski, M., Prescott,W.H., Savage C.J., and Johnston, M.J., 1990, Geodetic estimate of coseismic slip during the 1989 Loma Prieta, California, earthquake: Geophysical Research Letters, v. 17, p. 1437-1440.

Okada, Y., 1985, Surface deformation due to shear and tensile faults in a half-space: Bulletin of the Seismological Society of America, v. 75, p. 1135-1154.

Okal, E.A., 1988, Seismic parameters controlling far-field tsunami amplitudes: A review: Natural Hazards, v. 1, p. 67-96.

Satake, K., 1985, The mechanism of the 1983 Japan Sea earthquake as inferred from long-period surface waves and tsunamis: Physics of the Earth and Planetary Interiors, v. 37, p. 249-260, 1985.

Schwing, F.B., Norton, J.G., and Pilskaln, C.H., 1990, Earthquake and bay, response of Monterey Bay to the Loma Prieta earthquake: Eos, v. 71, p. 250-251.

Takahashi, R., 1942, On seismic sea waves caused by deformations of the sea bottom: Bulletin of Earthquake Research Institute, University of Tokyo, v. 20, p. 377-400.

Ward, S.N., 1982, Earthquake mechanisms and tsunami generation: The Kuril Islands earthquake of 13 October, 1963: Bulletin of the Seismological Society of America, v. 72, p. 759-777.

The Loma Prieta, California, Earthquake of October 17, 1989—Hydrologic Disturbances

STUART ROJSTACZER, *Editor*

STRONG GROUND MOTION AND GROUND FAILURE
THOMAS L. HOLZER, *Coordinator*

U.S. GEOLOGICAL SURVEY PROFESSIONAL PAPER 1551-E

UNITED STATES GOVERNMENT PRINTING OFFICE, WASHINGTON : 1994